Kinetik: Game Technology, Information System, Computer Network, Computing, Electronics, and Control
Journal homepage: http://kinetik.umm.ac.id
ISSN: 2503-2267
Vol. 9, No. 2, May 2024, Pp.139-148

Sensorless field-oriented control (FOC) using sliding mode observer for BLDC motor

Abdul Hafid Arif*[1], Muhammad Aziz Muslim[1], Erni Yudaningtyas[1]
Department of Electrical Engineering, Universitas Brawijaya, Malang[1]

Article Info
Keywords:
BLDC Motor, Field-Oriented Control, Sliding Mode Observer, Position Estimation, Motor Speed

Article history:
Received: December 22, 2023
Accepted: March 05, 2024
Published: May 31, 2024

Cite:
A. H. Arif, M. A. Muslim, and E. Yudaingtyas, "Sensorless Field-Oriented Control (FOC) using Sliding Mode Observer for BLDC Motor", KINETIK, vol. 9, no. 2, May 2024. Retrieved from https://kinetik.umm.ac.id/index.php/kinetik/article/view/1937

*Corresponding author.
Abdul Hafid Arif
E-mail address:
hfdism@gmail.com

Abstract
Motor Brushless Direct Current (BLDC) has become the preferred choice in various engineering applications. However, BLDC motor control involves high complexity, and motor performance depends on the control algorithms used. This research discusses the use of sensorless control methods, specifically the Sliding Mode Observer (SMO) for rotor position and speed estimation in BLDC motors within the context of Field-Oriented Control (FOC), validated through simulations using Matlab/Simulink. Simulation results indicate that SMO provides rapid dynamic response to current changes, albeit with slight delays at high speeds. Rotor position estimation with SMO is also reasonably accurate in both steady-state and transient conditions, affirming the iveness of SMO in sensorless control for BLDC motors. SMO can be experimentally implemented to enhance sensorless control in BLDC motors by reducing the cost of installing Hall sensors while maintaining comparable performance.

1. Introduction

The utilization of Brushless Direct Current (BLDC) motors is progressively widespread across various engineering applications, including robotics, electric vehicles, household appliances, power tools, and Unmanned Aerial Vehicles (UAVs). BLDC motors offer several advantages, such as high efficiency, elevated operating speed, a favorable torque-to-weight ratio, minimal maintenance requirements, and responsive dynamics [1]. Nevertheless, the control of BLDC motors involves intricate processes, and the performance of the motor is contingent on the chosen control algorithms [2].

Commonly used control methods for BLDC motors include trapezoidal scalar control and field-oriented control (FOC). Trapezoidal control has drawbacks such as torque ripple, limited speed range, and high noise [3]. FOC addresses these limitations by improving efficiency and maximizing torque per unit current [2]. Sensored FOC uses Hall sensors for accurate measurements [4][5], while sensorless FOC estimates rotor position using measurable system parameters [6-9].

The use of Hall sensors in BLDC motors to determine commutation angles poses several problems, including sensitivity to high temperatures, expensive sensor costs, installation difficulties, and sensor mounting errors [10]. Sensorless control, using Back Electro Motive Force (BEMF) as a reference, can overcome some of these issues [11].

In general, sensorless operations can be classified into two main categories: low-speed estimation and medium to high-speed estimation. In low-speed estimation, determining the rotor position involves the application of high and low-frequency injection methods, utilizing the specific effects of the motor in question [12][13].

On the other hand, for medium to high-speed operations, the commonly used estimation methods are Model Reference Adaptive System (MRAS) [14], extended Kalman filter (EKF) [15], Back-EMF estimation [16], and sliding mode observer (SMO) [17][18]. In research conducted by [19], SMO was developed within a stationary reference frame, replacing the sign function with saturation to reduce vibrations. Nevertheless, the inclusion of low-pass filtering remains crucial to dampen high-frequency noise.

Among the mentioned methods, SMO stands out as a viable option due to its ability to be implemented and offer robustness against uncertainties in parameters and measurement noise. In the context of FOC for BLDC motors, this paper proposes the utilization of the Sliding Mode Observer (SMO) for estimating rotor position and speed.

The Sliding Mode Observer (SMO) is employed to estimate the current, back-EMF, and position/speed of BLDC motors. This study introduces the SMO approach, which involves estimating both current and back-EMF to determine

the position/speed of the BLDC motor rotor. Additionally, Field-Oriented Control (FOC) outcomes obtained with Hall sensors serve as a benchmark for evaluating motor performance when employing SMO. The characterization of BLDC motor parameters is carried out using the STM32 Nucleo-F401RE board, ensuring a high level of simulation accuracy. The suggested control approach undergoes simulation in Matlab/Simulink to verify its effectiveness across different operating conditions.

2. Research Method

This research focuses on testing Sensorless Field-Oriented Control (FOC) with responses approaching the performance of a Brushless Direct Current (BLDC) motor using Hall sensors. FOC with the Sliding Mode Observer (SMO) method is employed for current, rotor position, and speed estimation. Subsequently, simulation tests are conducted to assess the performance of the responses generated by the BLDC. The response results present the performance of the BLDC using SMO and FOC, compared to the BLDC's performance when using Hall sensors. This study specifically emphasizes the analysis of the output performance of the sensorless BLDC using SMO and FOC. Literature studies are carried out in determining control design specifications and component specifications in a sequential and systematic manner. The flowchart guiding the research can be seen in Figure 1.

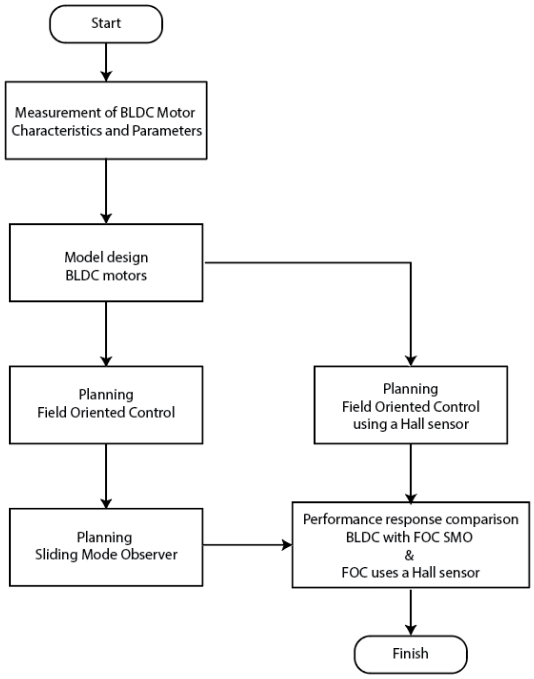

Figure 1. Research Stages

2.1 Mathematical Model of BLDC Motor

The development of a mathematical model for Brushless Direct Current (BLDC) motors assumes that the motor operates as a balanced three-phase system [20]. Therefore, the Equation 1 describing the machine are obtained in the abc reference frame, as outlined in reference [21].

$$\begin{bmatrix} Ua \\ Ub \\ Uc \end{bmatrix} = \begin{bmatrix} R_s & 0 & 0 \\ 0 & R_s & 0 \\ 0 & 0 & R_s \end{bmatrix} \begin{bmatrix} i_a \\ i_b \\ i_c \end{bmatrix} + \begin{bmatrix} L-N & 0 & 0 \\ 0 & L-N & 0 \\ 0 & 0 & L-N \end{bmatrix} \frac{d}{dt} \begin{bmatrix} i_a \\ i_b \\ i_c \end{bmatrix} + \begin{bmatrix} e_a \\ e_b \\ e_c \end{bmatrix} \quad (1)$$

Where $U_{a,b,c}$, $i_{a,b,c}$, , and $e_{a,b,c}$ represent the phase voltage, phase current, and the electromotive force (EMF) waveform of the phase, respectively, with the EMF waveform modeled as a trapezoidal function. R_s stands for stator resistance, while L and N denote the self-inductance and mutual inductance, respectively. Equation 2 depicts a model that relies on a trapezoidal EMF waveform. However, in the context of implementing Field-Oriented Control (FOC) to regulate the BLDC drive, a sinusoidal EMF waveform is obtained. Therefore, to enhance the precision of the BLDC motor model, it is recommended to utilize the α-β reference frame within the stationary reference frame, as suggested in Equation 2 [22].

$$L_s\left(\frac{di_\alpha}{dt}\right) = -R_s i_\alpha - e_\alpha + U_\alpha$$
$$L_s\left(\frac{di_\beta}{dt}\right) = -R_s i_\beta - e_\beta + U_\beta \quad (2)$$

Where

$$e_\alpha = -\omega_e \psi_{PM} \sin(\theta)$$
$$e_\beta = \omega_e \psi_{PM} \cos(\theta)$$

Where i_α, i_β, U_α, U_β,and e_α, e_β are the phase currents, phase voltages, and back-EMF in the stationary reference frame, respectively, R_s is the stator phase resistance, L_s is the stator phase inductance, ψ_{PM} is the flux linkage of the permanent magnet, ω_e is the electrical angular velocity, and θ is the electrical rotor position. From the back-EMF function in (1), it is evident that the back-EMF signal includes data on rotor speed and position. Therefore, once the back-EMF signal is estimated using the observer, information about the rotor's speed and position can be obtained.

The Equation 3 for electromagnetic torque (T_e) in the dq coordinates is determined by

$$T_e = \frac{3}{2} P(L_q . i_q - L_d i_d) - (C_L \omega_m - R_s i_d) \quad (3)$$

The formula for electromagnetic torque (T_e) in a synchronous motor in dq coordinates involving the number of poles (*P*), direct-axis inductance (L_q), and quadrature-axis inductance concerning the magnetic field (L_d) is derived from mathematical analysis and modeling of the synchronous motor in the dq coordinate system. In this equation, the direct-axis current (i_d) represents the component of current that flows along the direct axis of the motor, which affects the direct-axis inductance, while the quadrature-axis current (i_q) represents the component of current that flows along the quadrature axis, affecting the quadrature-axis inductance. The factor of 3/2 is associated with the transformation from a three-phase system to the dq coordinates. Additionally, the mechanical load (C_L) and stator resistance (R_s) also contribute to the overall electromagnetic torque.

2.2 Field-Oriented Control

Field-Oriented Control (FOC) is a technique employed to regulate a Brushless Direct Current (BLDC) motor by aligning the motor's torque and flux through the conversion of current from the stationary frame to the rotating frame. This process entails the detection of two-phase currents in the motor, followed by the application of Clark and Park transformations to convert these currents into the d and q frames [23].

The Clarke transformation is utilized to convert three-phase currents ($i_{a,b,c}$) from the stationary coordinate system into two-phase currents (i_α, i_β) in the rotating coordinate system. These two-phase currents are then used as inputs for the Park transformation. Meanwhile, the Park transformation is employed to convert the two-phase currents (i_α, i_β) obtained from the Clarke transformation into two-axis currents, namely the direct axis (d) and quadrature axis (q), enabling independent control of the motor's torque and flux. In the d-q frame, the d component represents the magnetic flux generated by the permanent magnet field, while the q component represents the flux generated by the current flowing through the motor winding's field coils.

Subsequently, the d and q-axis currents are compared to the reference flux and torque values. In the case of BLDC motor, where the flux remains constant due to the magnet, the reference flux is considered zero when controlling a BLDC. The system's torque reference is derived from the output of the speed controller and transformed into a q-axis current with the application of a scaling factor [24]. Figure 2 presents a simplified flowchart of the Field-Oriented Control (FOC) process for a BLDC motor.

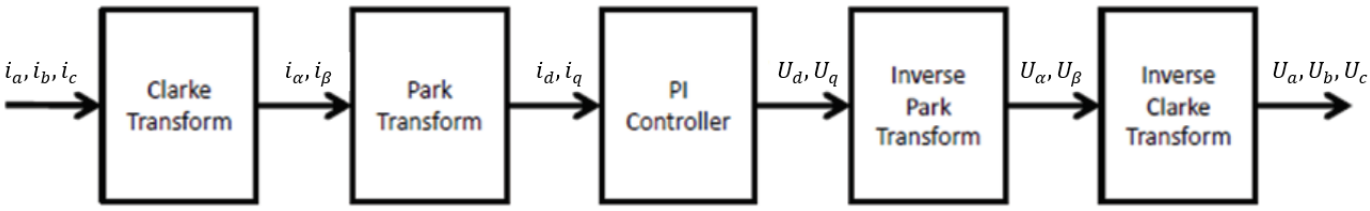

Figure 2. Flowchart of FOC

2.3 Sliding Mode Observer

The Field-Oriented Control (FOC) technique requires accurate rotor position information, which can be computed from the motor's back-EMF signal [25]. Back-EMF estimation, utilizing phase voltage and phase current measurements without neutral point connection, is incorporated into the SMO as depicted in Figure 3. The SMO, robust against parameter uncertainties, provides rotor position and speed estimates for precise control signals. The SMO ensures the accuracy of the system state estimation, regardless of measurable or unmeasurable conditions. This enhances the effectiveness of the FOC technique in dealing with parameter uncertainties and produces optimal control. The design of the SMO involves creating two observers: one for estimating current and another for estimating speed.

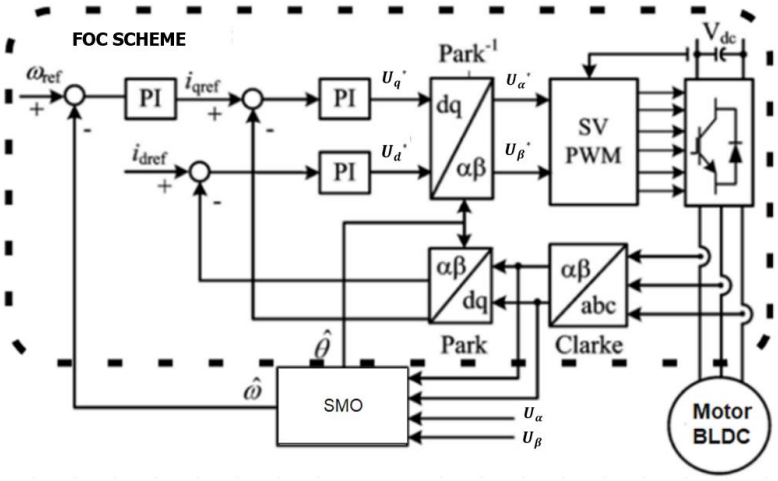

(a)

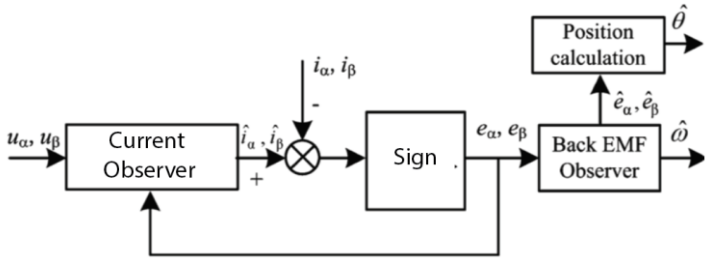

(b)

Figure 3. Flowchart of FOC

2.3.1 Current Observer

To design a current observer in MATLAB, the following equation is obtained:

$$\hat{I}_{(k+1)}=\hat{I}_{(k)} + sampling\ time * \hat{I}_{gradient(k)} \quad (4)$$

Equation 4 reflects the observation in the SMO, where the estimation of the current at the next iteration $(K+1)$ is calculated by adding the product of the sampling time and the current gradient $\hat{I}_{gradient(k)}$ at the current iteration to the estimation of the current at the previous iteration. This provides the system with the ability to dynamically adjust its current estimation based on the latest information of the current gradient, enabling a quick response to changes in the electric motor's conditions.

$$u(k) = k + sign(\hat{I}_{(k)} - I_{(k)}) \quad (5)$$

Equation 5 generates the control signal (u) used in the Sliding Mode Observer (SMO) control. This control signal aims to guide the estimated current $\hat{I}$ towards the correct direction or closer to the actual current, enabling the system to follow desired dynamics. The sign function returns the sign of each element in a vector. Specifically, if an element is positive, the result is 1; if negative, the result is -1; and if zero, the result remains zero. Therefore, $sign(\hat{I}_{(k)} - I_{(k)})$ produces a vector with elements that reflect the signs of the current differences in Equation 6.

$$sat(x)\begin{cases} -1, & x \le -1 \\ x, & -1 \le x \le 1 \\ 1, & x \ge 1 \end{cases} \quad (6)$$

Equation 7 is used in the Sliding Mode Observer (SMO) to update the current estimation at each time iteration, enabling the system to effectively track and respond to changes occurring within the motor system. Subsequently, the value of the control signal (u) is logged into the 'BackEMFCommandLog' data for the back EMF observer.

$$\hat{I}_{gradient(k)} = \frac{U_{(k)}{}'}{L_s} - \frac{\hat{I}_{(k)} x\, R_s}{L_s} - \frac{u_{(k)}}{L_s} \quad (7)$$

2.3.2 *Back-EMF Observer*

The back-EMF signal obtained from the current observer in Equation 8 is stored in 'BackEMFCommandLog' in MATLAB using the notation BackEMFCommandLog(i,1:2) = u;, denoted as e_{Cl}. To model the estimation process and the Butterworth filter on the back-EMF control voltage, the formula indicates the current time iteration, and the matrix element e_{Lpf} represents the filtered back-EMF. The values e'_{Cl} and e'_{Lpf} are respectively logging Back-EMF and Back-EMF after the transposed filter.

$$e_{Lpf(k)} = 0.00015705 * e'_{Cl(k)} + 0.00015705 * e'_{Cl(k-1)} + 0.99968 * e'_{Lpf(k-1)} \quad (8)$$

The estimation of electrical speed $\hat{w}_{(k)}$, defined as the difference between the electrical angles at iteration (k), can be formulated according to Equation 8 as follows:

$$\hat{w}_{(k)} = \hat{\theta}_{(k)} - \hat{\theta}_{(k-1)} \quad (9)$$

In Equation 9, $\hat{\theta}_{(k)}$ represents the estimated rotor angle at iteration k, and $\hat{\theta}_{(k-1)}$ represents the estimated rotor angle at the previous iteration. The rotor speed estimation $\hat{w}_{(k)}$ is obtained from the difference between the current and previous rotor angles, reflecting how fast the rotor moves between two consecutive samples. This speed information is used to regulate the current vector in the rotor coordinates, allowing precise and efficient control of torque and flux in sensorless FOC, achieving performance comparable to using a Hall effect sensor.

To ensure that the speed values remain within the range of $-\pi$ to π, phase wrap-around compensation is applied using an if-else condition. This approach adjusts $\hat{w}_{(k)}$ to compensate for phase shifts, ensuring that the speed estimation remains consistent and accurate within the specified range.

$$\hat{w}_{lpf(k)} = 0.00015705 * \hat{w}_{(k)} + 0.00015705 * \hat{w}_{(k-1)} + 0.99968 * \hat{w}_{lpf(k-1)} \quad (10)$$

Equation 10 represents a first-order Butterworth filter program for the estimation of electrical speed. The Butterworth filter is utilized to filter out noise or rapid fluctuations in the electrical speed estimation, providing a smooth response to changes in electrical speed. Where $\hat{w}_{lpf(k)}$ is the output result of the Butterworth filter at iteration k, $\hat{w}_{(k-1)}$ is the electrical speed at the previous iteration, and $\hat{w}_{lpf(k-1)}$ is the filter output at the previous iteration. To address the impact of speed changes on the electrical angle, which may occur due to significant changes in electrical speed, an equation is needed to correct the previously estimated electrical angle.

The estimation of the electrical angle (θ) plays a crucial role in achieving the desired performance. In BLDC motors, the accuracy of angle estimation is key to optimizing control and producing a fast and stable response. As an effective solution, the Sliding Mode Observer (SMO) method is employed to obtain real-time angle estimates. The equations involve the use of Butterworth filter results on the Back-EMF control voltage.

$$\dot{\theta}_{(k)} = \hat{\theta}_{(k)} + \text{atan}\,(\hat{w}_{lpf(k)}/(100 * \pi)) \quad (11)$$

In Equation 11, $\hat{\theta}_{(k)}$ is the variable used to store the estimated electrical angle of the motor. The term $atan\,(\hat{w}_{lpf(k)}/(100 * \pi)$ is added to $\hat{\theta}_{(k)}$ to compensate for the phase shift $\dot{\theta}_{(k)}$. This adjustment helps to correct any delays introduced by the filtering process. In this way, the estimated electrical angle after compensation will remain within a valid and expected range, avoiding discontinuities or errors caused by phase shifts.

3. Results and Discussion

Replicating the configuration illustrated in Figure 4 within the Matlab/Simulink environment serves as a validation for the SMO system. The regeneration of voltage components in the SMO involves space vector modulation, utilizing a low-voltage BLDC motor and the specified parameters in Table 1. This methodology guarantees a comprehensive assessment of the performance of the SMO system.

Table 1. BLDC Motor Specifications

Symbol	Parameter	Value
p	Number of pole pairs	2
Rs	Phase resistance	0.7Ω
Ls	Synchronous inductance	0.23 mH
λm	Permanent magnet flux linkage	59.2 mWb
Ke	Machine electrical constant	9.28 Vrms/kRPM
F	Friction	15.28 µN.m.s
I	Inertia	25.69 µN.m.s
N	Max Speed	1644 RPM

The Nucleo F401RE board facilitated the acquisition of motor parameters, as depicted in Table 1. Consequently, the precision of motor modeling in Matlab and Simulink simulations is notably high. In the FOC control strategy, the id current's reference value is established at zero. Within the Field-Oriented Control (FOC) strategy, the reference value for id current is set to zero, while a proportional-integral (PI) speed controller regulates the Id and Iq current references, as well as speed control. This approach ensures accurate representation and control of the motor system.

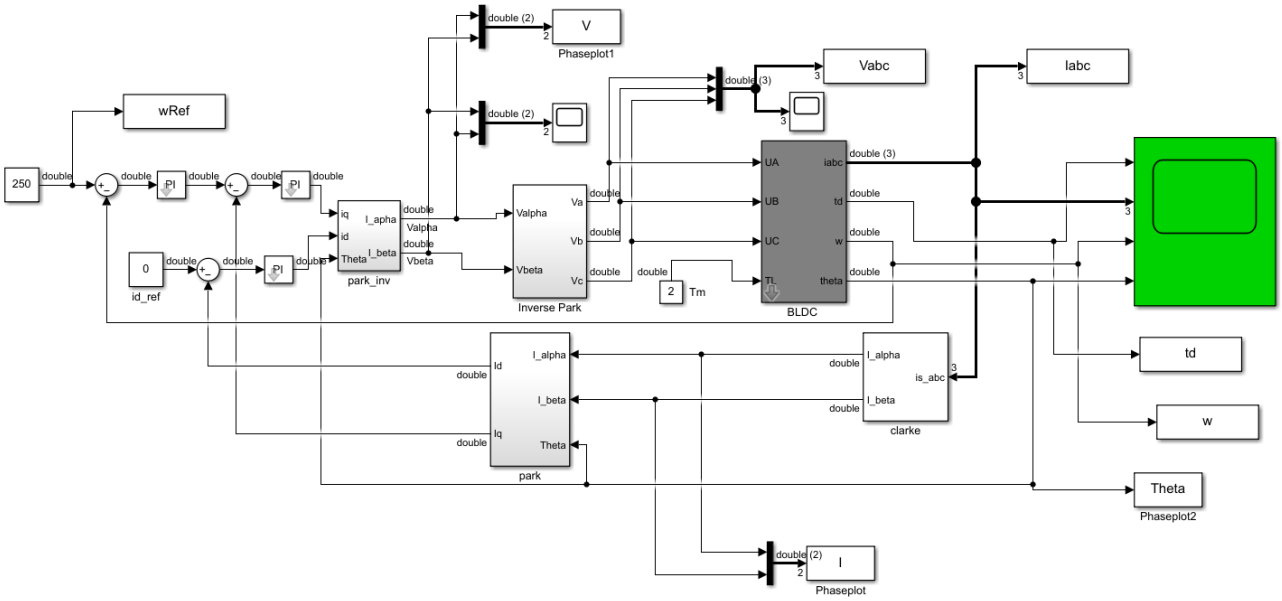

Figure 4. Field-Oriented Control System Block with Sliding Mode Observer

The simulation results for several constant speed variations with reference speeds set at 250, 500, 1000, and 1644 RPM, in accordance with the motor characteristics. Figure 5 displays the dynamic response of FOC with a Hall sensor on BLDC. For the rotor position response in FOC with SMO, in Figure 6, it is observed that the rotor position response experiences a delay of about 0.002s compared to FOC with a Hall sensor. This is because SMO requires estimating the rotor position based on mathematical models and voltage and current measurements. This estimation process takes extra time and is susceptible to disturbances or noise.

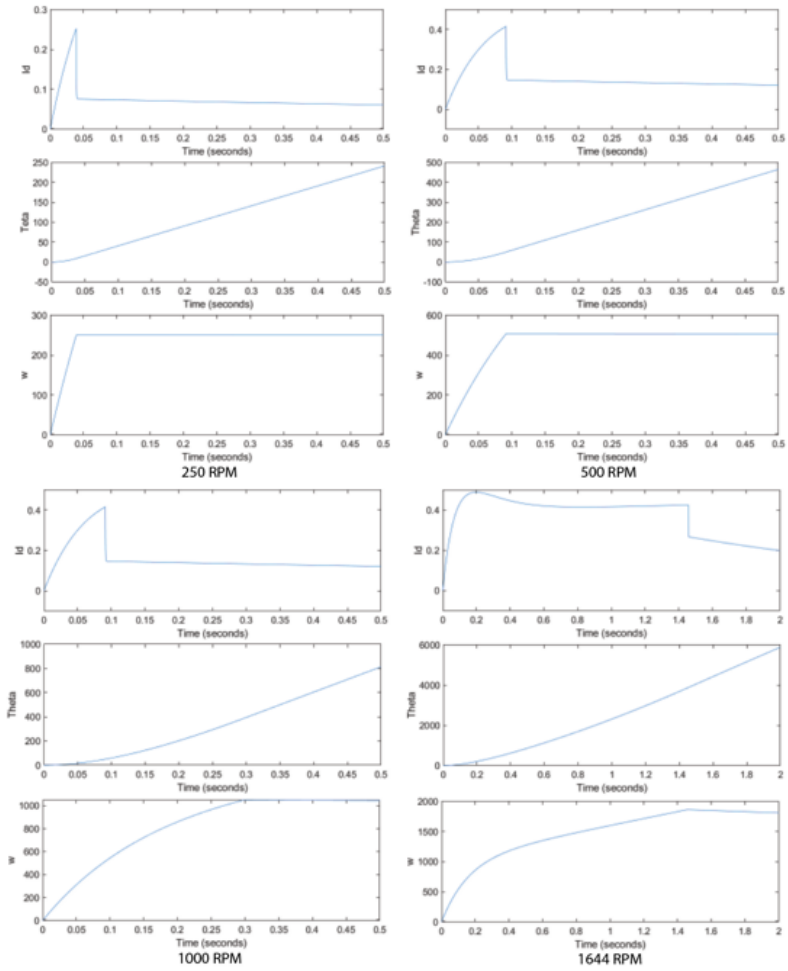

Figure 5. Id, theta, Speed Response on FOC is Censored to Changes in Speed Variations

In the speed response, theta angle, and Id value, there is also a delay in response due to the connection with rotor position identification. In FOC with SMO, the response indicates convergence to the actual speed, which takes less time at low speeds and becomes slower when the motor is given a high RPM reference. The speed, theta angle, and Id value responses exhibit similar response characteristics to the FOC response when provided with a Hall sensor.

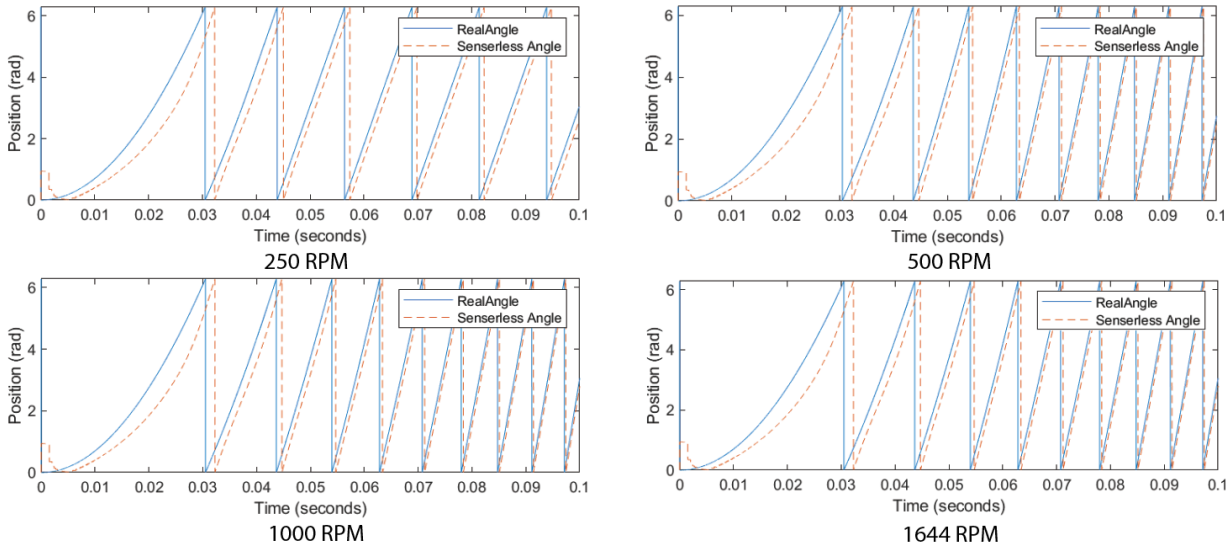

Figure 6. Comparison of Rotor Position Response on FOC with Hall Sensor and FOC with SMO

For the rotor position response of FOC with SMO, it is observed in Figure 6 that the rotor position response experiences a delay of approximately 0.002s compared to FOC with a Hall sensor. This delay is due to the fact that the SMO requires rotor position estimation based on a mathematical model and measurements of voltage and current. This estimation process takes extra time and is susceptible to disturbances or noise.

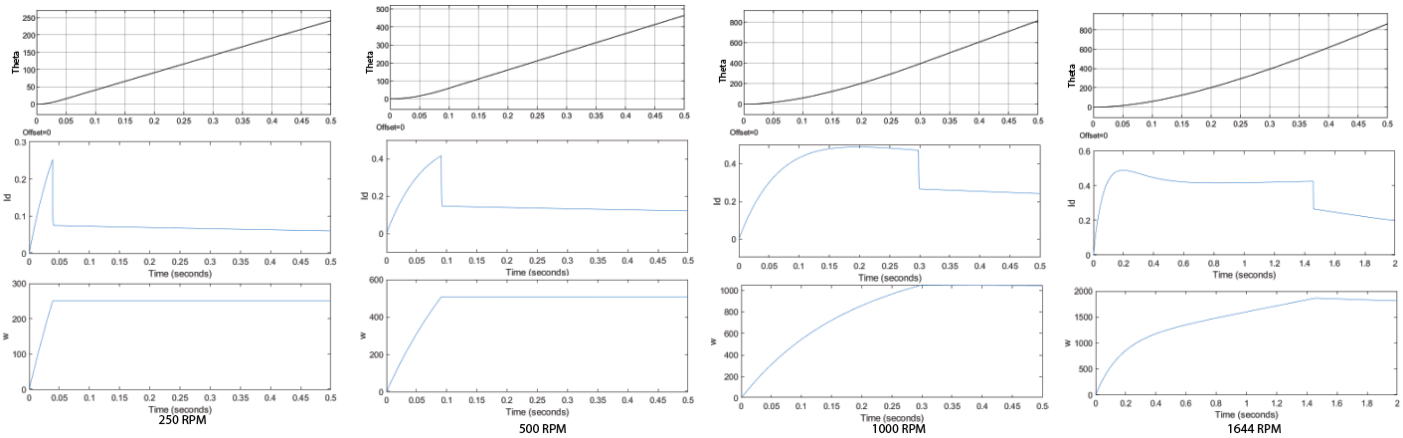

Figure 7. Theta, Id, and Speed Response at FOC with SMO to Changes in Speed Variations

In the context of position estimation, the Sliding Mode Observer (SMO) exhibits tracking accuracy that closely aligns with the actual position under both steady-state and transient conditions. The results presented in Figure 7 underscore the efficacy of the SMO, demonstrating a significant enhancement in the dynamic response of speed estimation, with performance comparable to Hall sensor-based control as illustrated in Figure 5. Phase delay compensation is typically employed to mitigate errors in speed estimation. Based on the outcomes, the proposed SMO proves to be suitable for experimental implementation in the sensorless control of BLDC motors.

4. Conclusion

In this study, the Sliding Mode Observer (SMO) was tested on a low-voltage Brushless DC (BLDC) motor using Matlab/Simulink with Field-Oriented Control (FOC). SMO provides fast dynamic responses to changes in current, although speed convergence is faster at low speeds. Sensorless control maintains stability even with small changes in current. In position estimation, SMO demonstrates accurate tracking compared to FOC with a Hall sensor in both steady-state and transient conditions. The research results affirm that SMO is effective and suitable for experimental implementation in sensorless control of BLDC motors.

References

[1] Mousmi, A., Abbou, A., & El Houm, Y. (2017, April). Trapezoidal control of Brushless DC motor based on DSP F28335. In 2017 International Conference on Wireless Technologies, Embedded and Intelligent Systems (WITS) (pp. 1-5). IEEE. https://doi.org/10.1109/WITS.2017.7934602

[2] Liu, C., & Luo, Y. (2017). Overview of advanced control strategies for electric machines. Chinese Journal of Electrical Engineering, 3(2), 53-61. https://doi.org/10.23919/CJEE.2017.8048412

[3] Golesorkhie, F., Yang, F., Vlacic, L., & Tansley, G. (2020). Field-Oriented control-based reduction of the vibration and power consumption of a blood pump. Energies, 13(15), 3907. https://doi.org/10.3390/en13153907

[4] Biniakos, N., & Iakovakis, V. (2019). Sensored Field-Oriented control of BLDC motor for pico satellite attitude control. International Journal of Innovative Science and Research Technology, 4.

[5] Amalia, Z., Khabib, A., Yudaningtyas, E., Machfuroh, T., Aini, F. A. N., & Rosady, S. D. N. (2023). Field-Oriented Control untuk Pengaturan Kecepatan Motor BLDC pada Sepeda Motor Listrik. Jurnal Elektronika dan Otomasi Industri, 10(1), 1-8. https://doi.org/10.33795/elkolind.v10i1.1977

[6] Song, X., Han, B., & Wang, K. (2018). Sensorless drive of high-speed BLDC motors based on virtual third-harmonic back EMF and high-precision compensation. IEEE Transactions on Power Electronics, 34(9), 8787-8796. https://doi.org/10.1109/TPEL.2018.2885031

[7] Wu, Z., & Wang, H. (2013, October). Sensorless control of the brushless DC motors based on TMS320F2812. In 2013 International Conference on Electrical Machines and Systems (ICEMS) (pp. 1184-1188). IEEE. https://doi.org/10.11142/jicems.2014.3.1.1

[8] Zhang, H., Tu, Y., & Wang, T. (2014, October). Sensor-less control for brushless DC motors based on hybrid sliding mode observer. In 2014 7th International conference on intelligent computation technology and automation (pp. 636-639). IEEE. https://doi.org/10.1109/ICICTA.2014.158

[9] Baratieri, C. L., & Pinheiro, H. (2013, October). An IF starting method for smooth and fast transition to sensorless control of BLDC motors. In 2013 Brazilian Power Electronics Conference (pp. 836-843). IEEE. https://doi.org/10.1109/COBEP.2013.6785212

[10] Song, X., Han, B., & Wang, K. (2018). Sensorless drive of high-speed BLDC motors based on virtual third-harmonic back EMF and high-precision compensation. IEEE Transactions on Power Electronics, 34(9), 8787-8796. https://doi.org/10.1109/TPEL.2018.2885031

[11] Chen, X., & Liu, G. (2019). Sensorless optimal commutation steady speed control method for a nonideal back-EMF BLDC motor drive system including buck converter. IEEE Transactions on Industrial Electronics, 67(7), 6147-6157. https://doi.org/10.1109/TIE.2019.2945282

[12] Song, X., Han, B., Zheng, S., & Chen, S. (2017). A novel sensorless rotor position detection method for high-speed surface PM motors in a wide speed range. IEEE Transactions on Power Electronics, 33(8), 7083-7093. https://doi.org/10.1109/TPEL.2017.2753289

[13] Gamazo-Real, J. C., Vázquez-Sánchez, E., & Gómez-Gil, J. (2010). Position and speed control of brushless DC motors using sensorless techniques and application trends. sensors, 10(7), 6901-6947. https://doi.org/10.3390/s100706901
[14] Ni, Y., & Shao, D. (2021, June). Research of Improved MRAS Based Sensorless Control of Permanent Magnet Synchronous Motor Considering Parameter Sensitivity. In 2021 IEEE 4th Advanced Information Management, Communicates, Electronic and Automation Control Conference (IMCEC) (Vol. 4, pp. 633-638). IEEE. https://doi.org/10.1109/IMCEC51613.2021.9482131
[15] Aishwarya, V., & Jayanand, B. (2016, March). Estimation and control of sensorless brushless dc motor drive using extended kalman filter. In 2016 International Conference on Circuit, Power and Computing Technologies (ICCPCT) (pp. 1-7). IEEE. https://doi.org/10.1109/ICCPCT.2016.7530343
[16] Chen, S., Liu, G., & Zhu, L. (2018). Sensorless startup strategy for a 315-kW high-speed brushless DC motor with small inductance and nonideal back EMF. IEEE Transactions on Industrial Electronics, 66(3), 1703-1714. https://doi.org/10.1109/TIE.2018.2838083
[17] Shah, V., & Vijayakumari, A. (2018, April). Field-Oriented control of surface mount permanent magnet synchronous machine with non linear observer for continuous rotor position estimation. In 2018 3rd International Conference for Convergence in Technology (I2CT) (pp. 1-6). IEEE. https://doi.org/10.1109/I2CT.2018.8529529
[18] Girija, P. K., & Prince, A. (2014, January). Robustness evaluation of SMO in sensorless control of BLDC motor under DTC scheme. In 2014 International Conference on Power Signals Control and Computations (EPSCICON) (pp. 1-6). IEEE. https://doi.org/10.1109/EPSCICON.2014.6887511
[19] Carey, K. D., Zimmerman, N., & Ababei, C. (2019). Hybrid Field-Oriented and direct torque control for sensorless BLDC motors used in aerial drones. IET Power Electronics, 12(3), 438-449. https://doi.org/10.1049/iet-pel.2018.5231
[20] Gambhir, R., & Jha, A. K. (2013). Brushless DC motor: Construction and applications. Int. J. Eng. Sci, 2(5), 72-77.
[21] Munoz-Gomez, G., Alanis, A. Y., & Rivera, J. (2018). Nested high order sliding mode controller applied to a brushless direct current motor. IFAC-PapersOnLine, 51(13), 174-179. https://doi.org/10.1016/j.ifacol.2018.07.274
[22] Qiao, Z., Shi, T., Wang, Y., Yan, Y., Xia, C., & He, X. (2012). New sliding-mode observer for position sensorless control of permanent-magnet synchronous motor. IEEE Transactions on Industrial electronics, 60(2), 710-719. https://doi.org/10.1109/TIE.2012.2206359
[23] Mehta, H., Joshi, V., & Kurulkar, P. (2016, June). Implementation issues of sliding mode observer for sensorless Field-Oriented control of PMSM using TMS320F2812. In 2016 IEEE Symposium on Sensorless Control for Electrical Drives (SLED) (pp. 1-6). IEEE. https://doi.org/10.1109/SLED.2016.7518798
[24] Sharifian, M. B. B., Herizchi, T., & Firouzjah, K. G. (2009, October). Field-Oriented control of permanent magnet synchronous motor using predictive space vector modulation. In 2009 IEEE Symposium on Industrial Electronics & Applications (Vol. 2, pp. 574-579). IEEE.
[25] Fakham, H., Djemaï, M., & Busawon, K. (2008). Design and practical implementation of a back-EMF sliding-mode observer for a brushless DC motor. IET Electric Power Applications, 2(6), 353-361. https://doi.org/10.1049/iet-epa:20070242